Surface-Enhanced Infrared External Reflection Spectroscopy at Low Reflective Surfaces and Its Application to Surface Analysis of Semiconductors, Glasses, and Polymers

Yuji Nishikawa and Kunihiro Fujiwara

Analytical Center, Konica Corporation, No. 1 Sakura-machi, Hino-shi, Tokyo 191, Japan

Ken-ichi Ataka and Masatoshi Osawa*

Department of Molecular Chemistry and Engineering, Faculty of Engineering, Tohoku University, Aoba, Aramaki, Aoba-ku, Sendai 980, Japan

A surface-enhanced infrared reflection spectroscopy has been developed for the characterization of thin organic films on low reflective substrates. The substrates we studied were BaF_2, Ge, microscope slide glass, and poly(acrylonitrile–butadiene–styrene) resin. The sensitivity of the reflection infrared spectroscopy at these surfaces is remarkably improved by evaporating very thin silver films on the sample surfaces. The same results were obtained also by casting thin organic films on metal-coated substrates. The improvement of the spectral sensitivity is due to the enhancement of the incident infrared field at the metal surfaces. We show that this technique is promising as a surface analytical tool for semiconductors and insulators. The optimum optical conditions to obtain the spectra are discussed experimentally and theoretically.

INTRODUCTION

Infrared spectroscopy is one of the most useful surface analytical tools. For metallic surfaces, the reflection technique so-called reflection–absorption spectroscopy (RAS)[1] has been widely used. However, RAS is not effective for surface studies of semiconductors and insulators because low reflection of these surfaces greatly reduces the sensitivity of this technique.

Infrared absorption of molecules is enhanced by an order of 10^1–10^3 when they are adsorbed on or near vacuum-evaporated very thin films of silver, gold, copper, and indium.[2-12] Hartstein et al.[2] found this surface-enhanced infrared absorption (SEIRA) phenomenon for the first time by using the attenuated-total-reflection (ATR) technique. They evaporated very thin (less than 10 nm) silver or gold film on a silicon ATR prism coated with molecular layers (metal-overlayer configuration). The metal films were not continuous but consisted of very small (<wavelength of light) islands (or particles). The same results were obtained with the metal-underlayer configuration, where the metal film was evaporated onto the prism and then a molecular layer was cast on it.

Recently, Ishida et al.[13,14] reported a metal-overlayer ATR technique that improves the sensitivity of surface infrared spectroscopy. This technique is very similar to the metal-overlayer technique by Hartstein et al. in experimental procedures except the metal thickness. The metal films they used were several tens of nanometers in thickness and were continuous. They showed that the electromagnetic fild in the organic layer sandwiched between a prism and metallic surface becomes very strong due to the interference of infrared radiation, resulting in strong absorption.[13] SEIRA also originates from an enhanced infrared electromagnetic field.[2-6,10-12] However, the electromagnetic enhancement is caused not by the interference of infrared radiation but through the excitation of plasma oscillation (or collective electron resonance) of the metal islands.[12] Osawa et al. showed experimentally[10] and theoretically[12] that the absorption enhancement by the electromagnetic mechanism is on the order of 10^1–10^2. Since the enhancement is remarkable for the molecules strongly chemisorbed onto the metal films, an increase in absorption coefficients caused by the chemisorption has been suggested to provide an additional enhancement.[10] However, this chemical mechanism is still unclear.

So far, most SEIRA spectra have been measured with the ATR methods. Recently, we obtained SEIRA spectra in transmission measurements.[8,10,11] Interestingly, however, Kamata et al.[6] did not observe SEIRA in external reflection measurements, where they evaporated a very thin silver film on a silver mirror coated with a Langmuir–Blodgett (LB) monolayer of stearic acid. The absence of SEIRA in their external reflection measurements is well expalined by the electromagnetic model associated with metal-island structure as follows. The metal islands can be modeled as oblate ellipsoids whose long axes are parallel to the substrate surface,[15,16] and the electromagnetic field along the long axes can excite the plasma oscillation in the visible and infrared regions.[15-17] When the substrate is highly reflective metals, however, the electromagnetic field is polarized normal to the substrate surface (and along the short axis of the ellipsoid)

(1) Greenler, R. G. *J. Chem. Phys.* **1966**, *44*, 310–315.
(2) Hartstein, A.; Kirtley, J. R.; Tsang, T. C. *Phys. Rev. Lett.* **1980**, *45*, 201–204.
(3) Hatta, A.; Suzuki, Y.; Suëtaka, W. *Appl. Phys. A* **1984**, *35*, 135–140.
(4) Osawa, M.; Kuramitsu, M.; Hatta, A.; Suëtaka, W.; Seki, H. *Surf. Sci.* **1986**, *175*, L787–L793.
(5) Suzuki, Y.; Osawa, M.; Hatta, A.; Suëtaka, W. *Appl. Surf. Sci.* **1988**, *33/34*, 875–881.
(6) Kamata, T.; Kato, A.; Umemura, J.; Takenaka, T. *Langmuir* **1987**, *3*, 1150–1154.
(7) Nakao, Y.; Yamada, H. *Surf. Sci.* **1986**, *176*, 578–592; *J. Electron Spectrosc. Relat. Phenom.* **1987**, *45*, 189–196.
(8) Nishikawa, Y.; Fujiwara, K.; Shima, T. *Appl. Spectrosc.* **1990**, *44*, 691–694; **1991**, *45*, 747–751.
(9) Nishikawa, Y.; Ito, Y.; Fujiwara, K.; Shima, T. *Appl. Spectrosc.* **1991**, *45*, 752–755.
(10) Osawa, M.; Ikeda, M. *J. Phys. Chem.* **1991**, *95*, 9914–9919.
(11) Osawa, M.; Ataka, K.; Ikeda, M.; Uchihara, H.; Nanba, R. *Anal. Sci.* **1991**, *7*, 503–506.
(12) Osawa, M.; Ataka, K. *Surf. Sci.* **1992**, *262*, L118–L122.
(13) Ishino, Y.; Ishida, H. *Appl. Spectrosc.* **1988**, *42*, 1296–1302.
(14) Khoo, C. G. L.; Ishida, H. *Appl. Spectrosc.* **1990**, *44*, 512–518.
(15) Yamaguchi, T.; Yoshida, S.; Kimbara, A. *Thin Solid Films* **1974**, *21*, 173–187.
(16) Marray, C. A. In *Surface Enhanced Raman Scattering*; Chang, R. K., Furtak, T. E., Eds.; Plenum Press: New York, 1982.
(17) Osawa, M.; Suëtaka, W. *Surf. Sci.* **1987**, *186*, 583–600.

0003-2700/93/0365-0556$04.00/0

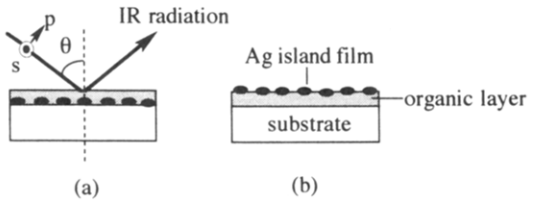

Figure 1. Metal-underlayer (a) and -overlayer (b) configurations.

in the reflection conditions.[1,18,19] Therefore, the plasma oscillation is not excited and SEIRA does not occur.

In the present study, we show that SEIRA is observed even with the external reflection method if the substrate is transparent or translucent. This is because the electromagnetic field has both parallel and normal components at such low reflective surfaces.[18,19] The observed band intensity depends upon polarization and the incident angle of the infrared radiation. Combined with a theoretical calculation using Fresnel's equations and our electromagnetic model of SEIRA,[12] the optimum optical conditions for obtaining the spectra are discussed. In addition, we show that metal-overlay reflection SEIRA spectroscopy is promising as a surface analytical technique for semiconductors, glasses, and polymers. The use of this technique allows us to achieve monolayer sensitivity. The usefulness of this technique is given for, as examples the analyses of a LB monolayer on glass and a "mold-releasing agent" on poly(acrylonitrile–butadiene–styrene) (ABS) resin. The practical aspects and limitations of this technique are also discussed.

EXPERIMENTAL SECTION

We carried out the external reflection SEIRA experiments both with metal-overlayer and -underlayer configurations. The two configurations are shown in Figure 1. The substrates used were BaF_2 (20 × 20 × 4 mm), Ge (20 × 20 × 4 mm), microscope slide glass (20 × 20 × 1 mm), and ABS resin (20 × 20 × 2 mm). The substrate plates except the ABS resin plate were washed first with ethanol and then with chloroform to remove surface contaminants. The ABS resin plate was cleaned only with ethanol. In metal-underlayer configuration experiments, silver films were evaporated on the substrates from a tungsten basket by thermal heating in a JEOL JEE 4C vacuum evaporator under a base pressure below 5×10^{-5} Torr. The metal deposition was monitored and controlled with a quartz thickness monitor (Maxtek, Inc.). Then, thin films of *p*-nitrobenzoic acid (PNBA) or poly(dimethylsiloxane) (PDMS) were cast on the silver-coated substrates by dropping their dilute ethanol or 2-butanone solution with a microsyringe. The solvents were allowed to evaporate in the air.

In the metal-overlayer configuration, the organic films were cast on the substrates with the same procedure described above and then metal films were evaporated on top of the orgnaic layer. A LB monolayer of poly(*n*-dodecylacrylamide) was formed on water and was transferred onto a glass plate with the procedures reported by Miyashita et al.[20] All the chemicals were reagent-grade and were used without further purification.

The metal thickness quoted in the present paper is the mass thickness, d_{mass}, unless otherwise cited. The thickness of the organic films was estimated from the volume and concentration of the solution used by assuming densities of the bulk crystals (1.61 and 0.97 g/cm^3 for PNBA and PDMS, respectively).

Infrared spectra were recorded on a Nicolet 60SX FT-IR spectrometer equipped with a wide-band MCT detector at a resolution of 4 cm^{-1} by co-adding 1024 scans. The angle of incidence (θ) was changed between 20 and 80° using a variable-angle reflection attachment Seagull (Harrick Scientific Corp.). A p- or s-polarized infrared beam was incident on the surface through a wire grid polarizer (Specac, England). Background spectra were measured before the deposition of molecules (in metal-underlayer configuration) or before the deposition of silver (in metal-overlayer configuration). All the spectra are shown by absorbance unit defined as $-\log(R/R_0)$, where R_0 and R are reflectances of the sample plate before and after the molecular layer (or silver film) is deposited, respectively.

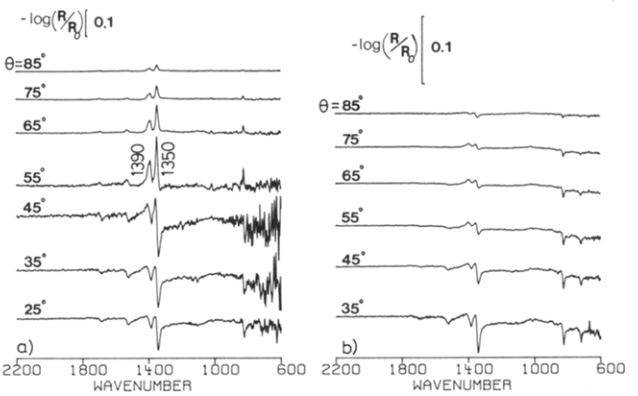

Figure 2. Silver-underlayer reflection SEIRA spectra of a 4-nm-thick PNBA film on BaF_2 for p- and s-polarizations (a and b, respectively). The thickness of the silver underlayer is 5 nm. The numbers in the figure denote the incident angle (θ).

The structure of the silver films evaporated on BaF_2 and Ge were observed with a Hitachi Model 3-800 field-emission scanning electron microscope (SEM) at an accelerating voltage of 200 kV.

RESULTS AND DISCUSSION

A. Metal-Underlayer Configuration. We first carried out the experiments with metal-underlayer configuration because structures of thin silver films evaporated on glasses, Ge, and quarts have been well studied.[16,21,22] The shape and size of the metal islands must be defined for simulations of SEIRA spectra described below. To simplify the calculation, BaF_2 and Ge were used as model substrates because their refractive indices are real and almost constant in the infrared region (n = 1.42 and 4.0, respectively).

Figure 2 shows the p- and s-polarized reflection spectra of a 4-nm-thick PNBA film on a 5-nm-thick silver film evaporated on a BaF_2 plate. The spectra were obtained at various incident angles shown in the figure. The peak positions of the bands observed here are in good agreement with those observed in the ATR[3,5,9] and transmission[8,10,11] SEIRA spectra. The C=O stretching band of PNBA is missing in the expected frequency region around 1700 cm^{-1} and the symmetric COO^- stretching band is observed at 1390 cm^{-1}, indicating that PNBA was adsorbed onto the sample surface through the carboxyl group and dissociated proton. The proton dissociation occurs only for the first monolayer at silver surfaces.[10] We show below that the dissociation does not occur on the BaF_2 surface. The strongest band at 1350 cm^{-1} is assigned to the symmetric NO_2 stretching mode. All the bands, except the weak antisymmetric NO_2 stretching band at 1527 cm^{-1}, are attributed to the A_1 modes of *p*-nitrobenzoate ($PNBA^-$).[23] Since the enhanced electromagnetic field is normal to the metal surface and $PNBA^-$ is adsorbed with its C_2 axis normal to the surface, the B_1 and B_2 modes having dipole oscillations normal to the C_2 axis are almost missing.[10,11]

(18) Hansen, W. N. *Advances in Electrochemistry and Electrochemical Engineering*; Delahay, P., Tobias, C. W., Eds.; Wiley Interscience: New York, 1973; Vol. 9, Chapter 1.
(19) MacIntyre, J. D. E. In *Advances in Electrochemistry and Electrochemical Engineering*; Delahay, P., Tobias, C. W., Eds.; Wiley Interscience: New York, 1973; Vol. 9, Chapter 2.
(20) Miyashita, T.; Mizuta, T.; Matsuda, M. *Br. Polym. J.* **1990**, *22*, 327–331.
(21) Senett, R. S.; Scott, G. D. *J. Org. Soc. Am.* **1950**, *40*, 203–211.
(22) Garoff, S.; Stephens, R. B.; Hanson, C. D.; Sorenson, G. K. *Opt. Commun.* **1982**, *41*, 257–261.
(23) Ernstbrunner, E. E.; Girling, R. B.; Hester, R. E. *J. Chem. Soc., Faraday Trans. 2* **1978**, *74*, 1540–1549.

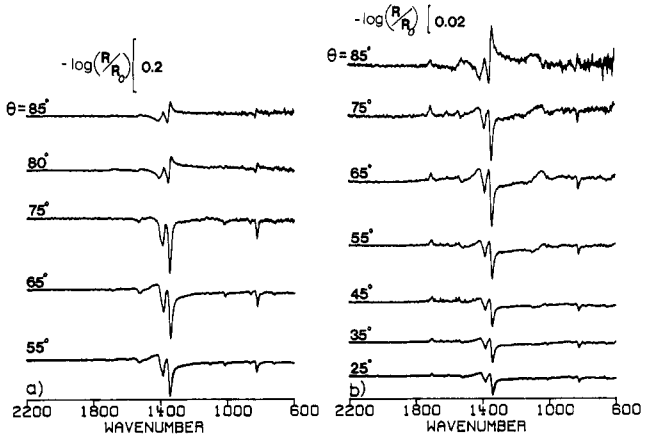

Figure 3. p-polarized silver-underlayer reflection SEIRA spectra of 4-nm-thick PNBA films on BaF_2 (a) and Ge(b). The thickness of the silver underlayer is 10 nm (a) or 5 nm (b).

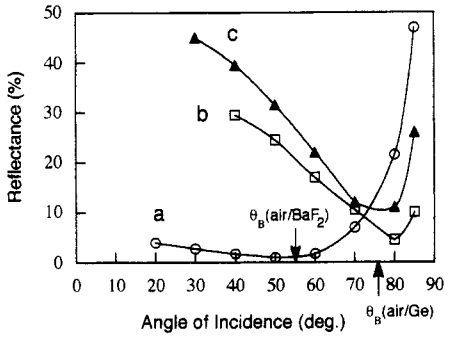

Figure 4. Reflectance of the silver-underlayer samples used in Figures 2 and 3 at 1600 cm^{-1} for p-polarization as a function of θ. The substrates are BaF_2 (a, b) and Ge (c). The metal thickness is 5 nm (a, c) or 10 nm (b). θ_B are Brewster angles of the air/BaF_2 and air/Ge interfaces (54.85 and 75.96°, respectively).

We note that the reflection SEIRA spectra are slightly different from the previously reported transmission and ATR SEIRA spectra of the molecule.[3,5,8-11] In the latter two spectra, the vibrational modes were observed as up-going bands (normal absorption). In the s-polarized reflection SEIRA spectra in Figure 2, however, absorption is negative. The peak intensities decrease as θ increases. We see two positive absorption bands at 1400 and 1360 cm^{-1} for θ = 55–75°, but these bands arise due to distortion of the 1390- and 1350-cm^{-1} bands as described below. For p-polarization, both negative and positive absorption bands are observed, and show dependence on θ. Absorption is negative at $\theta \leq 45°$ and is positive at $\theta \geq 55°$.

The critical incident angle where the spectrum is reversed up and down shifts to a higher angle around 80° for a 10-nm-thick silver film on BaF_2, as shown in Figure 3a. The critical angle depends also on the substrate. For a 5-nm-thick silver film on Ge, the reversion of the spectrum is observed around 80°, as shown in Figure 3b. Absorption for s-polarization was always negative and was smaller than that for p-polarization independent of metal-film thickness and substrate (not shown).

Curve a in Figure 4 shows the reflectance of the sample used in Figure 2 at 1600 cm^{-1} for p-polarization plotted versus θ. An aluminum mirror was used as a reference. A minimum is observed around the Brewster angle of the air/BaF_2 interface ($\theta_B = \tan^{-1} n = 54.85°$). Low reflectance of the substrate around θ_B results in a decrease of signal-to-noise (S/N) ratios of the p-polarized spectra (see Figure 2). The reflectance for s-polarization was higher than that for p-polarization and increased monotonously as θ increases (not shown). We see that the up-and-down reversion of the spectra in Figure 2a

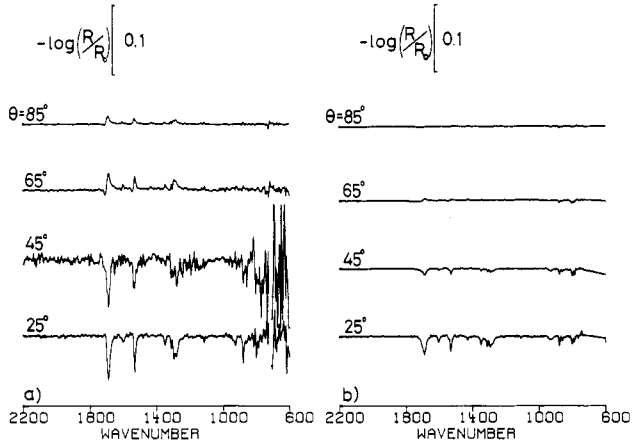

Figure 5. Infrared reflection spectra of a 40-nm-thick PNBA film on BaF_2 without a silver film for p- and s-polarizations (a and b, respectively).

occurs around θ_B. It is also the case for the samples used in Figure 3. The Brewster angles (more exactly, pseudo-Brewster angles) are about 80° for the 10-nm-thick silver-coated BaF_2 and the 5-nm-thick silver-coated Ge (curves b and c in Figure 4, respectively). At incident angles less than 80°, only the negative absorption bands are observed for p-polarization in Figure 3.

For comparison, we measured the external reflection spectra of the organic film of the same thickness deposited on BaF_2 (without a metal film) but no absorption was observed. We show in Figure 5 the p- and s-polarized reflection spectra of a 10-times thicker (40-nm) PNBA film on BaF_2. The C=O stretching vibration is observed strongly at 1690 cm^{-1}, but the symmetric COO^- stretching band is not present in these spectra. This result indicates that the proton dissociation does not occur on BaF_2. Although the spectrum is different from the SEIRA spectra, the θ and polarization dependence are the same. The negative absorption bands are seen at all θ for s-polarization and at $\theta < \theta_B$ for p-polarization. The same θ and polarization dependences have been reported also on water[24] Si,[25] and Cu_2S[26] substrates. Therefore, the abnormal negative absorption in the SEIRA spectra is not an inherent nature of SEIRA but is due to the influence of the substrate.

If the absorption coefficients of the symmetric NO_2 bands of PNBA and the chemisorbed $PNBA^-$ are assumed to be equal, the absorption enhancement by the presence of 5-nm-thcik silver film is calculated to be a factor of about 50 on the BaF_2 substrate from a comparison of the spectra in Figures 2 and 5 by taking account of the difference in thickness of the organic layers. The enhancement factor on Ge substrate was estimated to be about 20 by the same procedures.

B. Simulation of Reflection SEIRA Spectra. Negative absorption in external reflection spectroscopy at transparent and translucent substrates has been simulated by applying the Fresnel equations[18,19] to three-phase systems of air/organic layer/substrate.[24-26] We carried out the same calculations for a four-phase system of air/organic layer/silver/substrate by using optical constants of bulk silver. However, the observed spectra were not simulated.

It is well-known that very thin silver films evaporated on substrates such as glasses, quartz, and Ge consist of islands.[16,21,22] Figure 6 shows typical SEM images of our 10-nm-thick silver films evaporated on BaF_2 and Ge. The metal films consist of metal particles 20–100 nm in size, some of which are connected with the surrounding particles. The

(24) Dluhy, R. A. *J. Phys. Chem.* **1986**, *90*, 1373–1379.
(25) Allara, D. L.; Baca, A.; Pryde, C. A. *Macromolecules* **1978**, *11*, 1215–1220.
(26) Mielczarski, J. A.; Yoon, R. J. *J. Phys. Chem.* **1989**, *93*, 2034–2038.

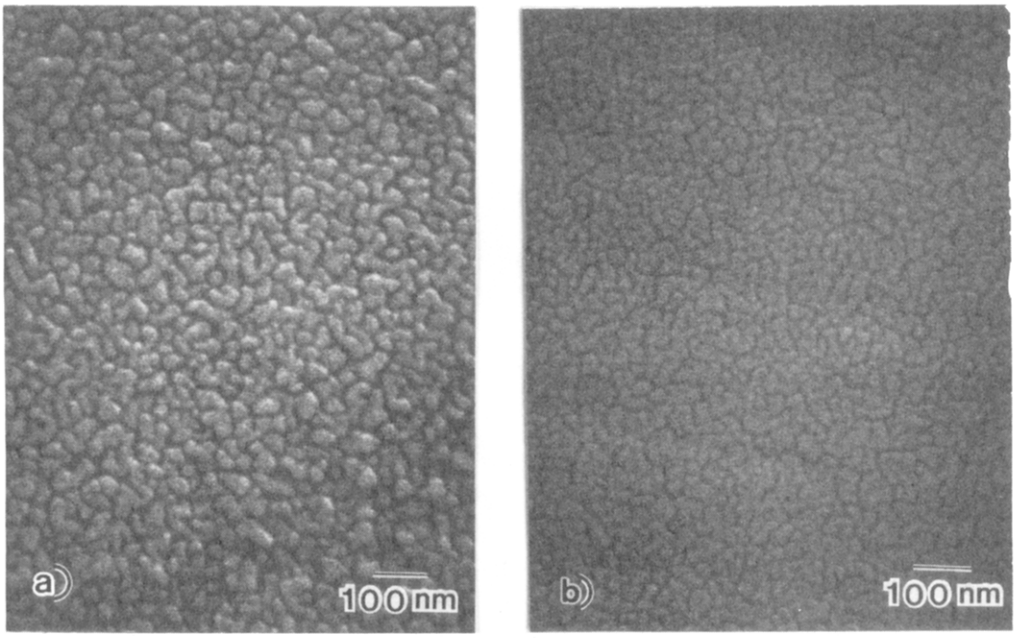

Figure 6. Scanning electron micrographs of 10-nm-thick silver films evaporated on BaF_2 (a) and Ge (b).

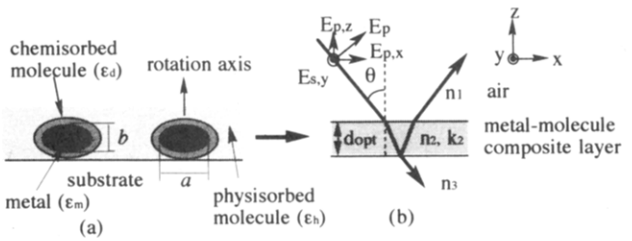

Figure 7. Rotational ellipsoid model of a metal-island film (a) and hypothetical plane-parallel film model (b). The aspect ratio of the ellipsoid is defined as $\eta = a/b$, where a and b represent the radii along the long and short axes of the ellipsoid, respectively. The subscripts of electromagnetic field E denote the polarization (p or s) and oscillating direction (x, y, z).

metal particles on Ge are slightly smaller than those on BaF_2. Since the islands are smaller than the wavelength of light, however, the island films can be modeled by plane-parallel layers consisting of metal particles and host medium (molecules and/or air) with an effective optical thickness d_{opt} as shown in Figure 7.[4,5,17] Under this assumption, we calculate the reflectance of the three-phase system of air (phase 1)/composite layer (phase 2)/substrate (phase 3) by using Fresnel's formula. We define the optical constants of these phases by $n_1(=1)$, $\hat{n}_2(=n_2 + ik_2)$, and n_3, respectively. We also define x, y, and z axes as shown in the figure.

The optical constant of the composite layer is distinctively different from that of the bulk metal[15,27] and can be estimated with effective medium theories.[15,28] According to the Maxwell-Garnett model,[28] the effective (or spatially averaged) dielectric function of the composite film, ϵ_2 $(=\hat{n}_2^2)$, is written as

$$\epsilon_2 = \epsilon_h\left(\frac{3 + 2F\alpha}{3 - F\alpha}\right) \tag{1}$$

Here ϵ_h is the dielectric constant of the host medium, F is the filling factor of the metal defined by $F = d_{mass}/d_{opt}$,[27] and α is the polarizability of the metal particles.

The polarizability is a function of the shape and size of the particles.[15,29] According to the previous theoretical studies,[15,16,29] we model the metal islands as uniformly sized rotational ellipsoids (Figure 7a). The rotation axes are taken to be perpendicular to the substrate. Each ellipsoid is defined by volume V_1, dielectric function of the bulk metal ϵ_m, and aspect ratio η $(=a/b; a$ and b are radii along the long and short axes of the ellipsoid, respectively, as shown in Figure 7a). Optical properties depend also on the aggregation density of the islands,[15] which is incorporated into the calculation through F. The chemisorbed $PNBA^-$ layer is modeled by a layer with dielectric function ϵ_d surrounding each silver particle. Since the SEIRA spectra are dominated by the bands of $PNBA^-$ and did not change greatly when the physisorbed free acid was washed out from the surface with acetone, we take ϵ_h in eq 1 as 1 (air) for the sake of simplicity. The polariability of a metal particle surrounded by the dielectric layer is given[29] by

$$\alpha_{\parallel,\perp} = \{[(\epsilon_d - 1)[\epsilon_m L_1 + \epsilon_d(1 - L_1)] + Q(\epsilon_m - \epsilon_d) \times [\epsilon_d(1 - L_2) + L_2]]/[[\epsilon_d L_2 + (1 - L_2)][\epsilon_m L_1 + \epsilon_d(1 - L_1)] + Q(\epsilon_m - \epsilon_d)(\epsilon_d - 1)L_2(1 - L_2)]\}_{\parallel,\perp} \tag{2}$$

where the subscripts $\parallel$ and $\perp$ refer to the applied field being parallel or perpendicular to the substrate, respectively. Q is the volume ratio of the core and coated ellipsoids $(=V_1/V_2)$. The thickness of the molecular layer, d_{mol}, is incorporated into the calculation through Q. The different aspect ratios of the core and coated spheroids are represented by the different depolarization factors L_1 and L_2, respectively. The depolarization factors are tabulated in ref 30 as a function of η and are normalized to $L_\perp + 2L_\parallel = 1$.

The dielectric function of silver can be calculated by the Drude free-electron theory given by

$$\epsilon_m = 1 - \frac{\omega_p^2}{\omega(\omega + i/\tau)} \tag{3}$$

We use parameters obtained by Johnson and Christy[31] ($\omega_p = 1.38 \times 10^{16}$ s^{-1}, and $\tau = 3.1 \times 10^{-14}$ s). The surface molecule is modeled as a combination of Lorentz oscillators, whose

(27) Malé, D. *J. Phys. Radium* **1964**, *25*, 74–77.
(28) Niklasson, G. A.; Granqvist, C. G. *J. Appl. Phys.* **1984**, *55*, 3382–3410.
(29) Eagen, C. F. *Appl. Opt.* **1981**, *20*, 3035–3042.
(30) Stoner, E. C. *Philos. Mag. 7*, **1945**, *36*, 803–820.
(31) Johnson, M. R.; Christy, R. W. *Phys. Rev. B* **1972**, *6*, 4370–4379.

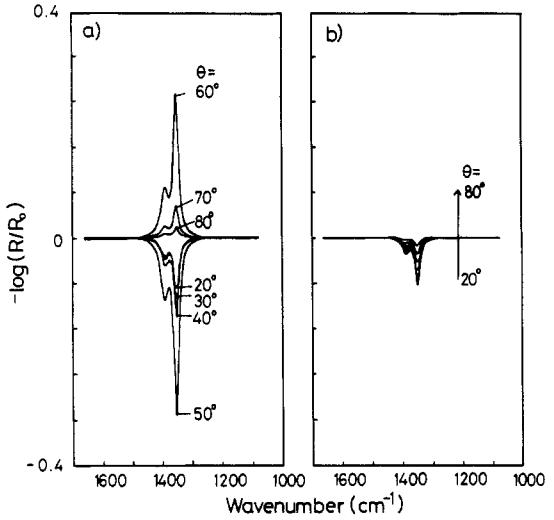

Figure 8. Simulated reflection SEIRA spectra of a model molecular layer (d_{mol} = 1 nm) on a silver film (d_{mass} = 5 nm, F = 0.6, a = 20 nm, η = 2) on BaF_2 for p- and s-polarizations (a and b, respectively).

absorption coefficients are given by

$$k_d(\omega) = \frac{k_{max}/(\gamma/2)^2}{(\omega_0 - \omega)^2 + (\gamma/2)^2} \tag{4}$$

where ω_0 is a peak frequency. The real part of the complex refractive index ($\epsilon_d^{1/2} = \hat{n}_d = n_d + ik_d$) can be calculated by the Kramers–Kronigh transformation

$$n_d(\omega) = n_\infty + \frac{2}{\pi}\int_0^\infty \frac{\omega k_d(\omega)\, d\omega}{(\omega^2 - \omega_0^2)} \tag{5}$$

We assume that the adsorbed molecule has two bands at 1390 and 1350 cm^{-1} to simulate the 1300–1500-cm^{-1} range of the observed spectra. The width (fwhm = γ) and k_{max} are arbitrarily assumed to be 30 cm^{-1} and 0.15 for the 1390-cm^{-1} band and 20 cm^{-1} and 0.5 for the 1350-cm^{-1} band. The refractive index at a frequency far from the absorptions, n_∞, is tentatively assumed to be 1.5.

As can be seen from eq 2, the optical response of the metal–molecule–air composite layer is anisotropic ($\hat{n}_{2,\parallel} \neq \hat{n}_{2,\perp}$) unless η = 1. To take account of the anistropy, we calculate the reflectance by using Fresnel's equations modified by Mielczarski and Yoon.[26] The change in the reflectance of the metal-coated substrate by the presence of the molecule is given in absorbance unit as

$$A_{s,y} = -\frac{16\pi}{\ln 10}\left[\frac{\cos\theta}{n_3^2 - 1}\right]\frac{n_{2\parallel}k_{2\parallel}d_{opt}}{\lambda} \tag{6a}$$

for s-polarization and

$$A_{p,x} = -\frac{16\pi}{\ln 10}\left[\frac{\cos\theta}{\xi_3^2/n_3^4 - \cos^2\theta}\right]\left[-\frac{\xi_3^2}{n_3^4}\right]\frac{n_{2\parallel}k_{2\parallel}d_{opt}}{\lambda} \tag{6b}$$

$$A_{p,z} = -\frac{16\pi}{\ln 10}\left[\frac{\cos\theta}{\xi_3^2/n_3^4 - \cos^2\theta}\right]\frac{\sin^2\theta}{(n_{2\perp}^2 + k_{2\perp}^2)^2}\frac{n_{2\perp}k_{2\perp}d_{opt}}{\lambda} \tag{6c}$$

for p-polarization, where $\xi_3 = (n_3^2 - n_1^2\sin^2\theta)^{1/2}$ and λ is the wavelength. The second subscripts of A (x, y, and z) represent the x, y, and z components of the incident electromagnetic field, respectively. The net change in absorbance for p-polarization is given by $A_{p,x} + A_{p,z}$.

Figure 8 shows the simulated reflection SEIRA spectra for the model molecular layer of 1 nm in thickness deposited on a 5-nm-thick silver film on BaF_2. We assumed F = 0.6 from the F versus d_{mass} curve obtained experimentally by Malé.[27] Since we could not obtained SEM images of our 5-nm-thick silver film on BaF_2 due to charge-up of the sample, we assumed a = 20 nm and η = 2.0 from the SEM observation by Garoff et al.[22] As is seen in the figure, the absorption bands are always negative for s-polarization independent of θ. For p-polarization, the absorption is negative at $\theta \leq 50°$ and positive at $\theta \geq 60°$.

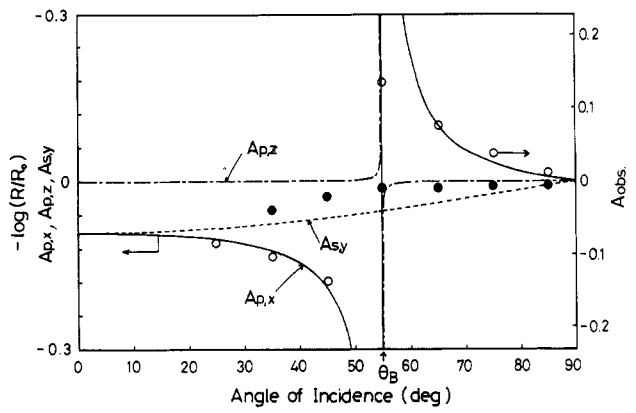

Figure 9. Calculated absorbance for a model organic layer (n_m = 1.5 and k_m = 0.5 at 1350 cm^{-1}; d_{mol} = 1 nm) on a silver-island film (d_{mass} = 5 nm, F = 0.6, a = 20 nm, η = 2) on BaF_2 as a function of incident angle θ. The open and closed circles are the peak intensities of the 1350-cm^{-1} band in Figure 2 for p- and s-polarizations, respectively. θ_B is the Brewster angle of the air/BaF_2 interface (=54.85°).

To see the θ and polarization dependence of the SEIRA spectra in more detail, three components of the absorption ($A_{p,x}$, $A_{p,z}$, and $A_{s,y}$) for the 1350-cm^{-1} band are compared in Figure 9 as a function of θ. The $A_{s,y}$ component (dashed line) is always negative and approaches zero as θ increases. The $A_{p,x}$ component (solid line) is negative at $\theta < \theta_B$ and positive at $\theta > \theta_B$. The $A_{p,z}$ component (dot-dashed line) is almost zero except around θ_B due to the following two reasons. First, the plasma resonance is not excited with the electromagnetic field normal to the long axis of the metal particle,[4,16,17] which is incorporated into the present calculation by $L_\perp > L_\parallel$. Second, z-component of the electromagnetic field ($E_{p,z}$, see Figure 7) is greatly damped in the composite layer due to the interference between the incident and reflected radiations.[4,5] The open and closed circles in the figure are the experimentally observed θ dependence of the peak intensity at 1350 cm^{-1} in Figure 2 (for p- and s-polarization, respectively). Since the absorption coefficient of the molecule is assumed arbitrarily in the calculation, there is a difference in magnitude between calculated and experimental absorbance values. However, the observed θ and polarization dependence are well simulated.

A calculation without a metal film ($\epsilon_h = \epsilon_d$ and F = 0) provided the same spectra as in Figure 8, but the peak intensity was about 15 times smaller. Therefore, the enhancement factor caused by the electromagnetic mechanism is estimated to be 15. Since the enhanced electromagnetic field around metal particles is normal to their local surfaces, however, the observable enhancement factor greatly depends on the orientation of surface molecules and the symmetries of molecular vibrations.[10-12] This is well demonstrated in Figures 2 and 3, where only the A_1 modes are enhanced. If the dipole-oscillating direction of a molecular vibration is normal to the metal surface, the enhancement factor of 15 must be multiplied by 3.[12] The estimated enhancement factor of 45 (=15 × 3) is in good agreement with the experimentally observed enhancement factor of about 50 for the symmetric NO_2 mode.

The observed reflection SEIRA spectra are slightly distorted especially around θ_B and resemble derivative spectra

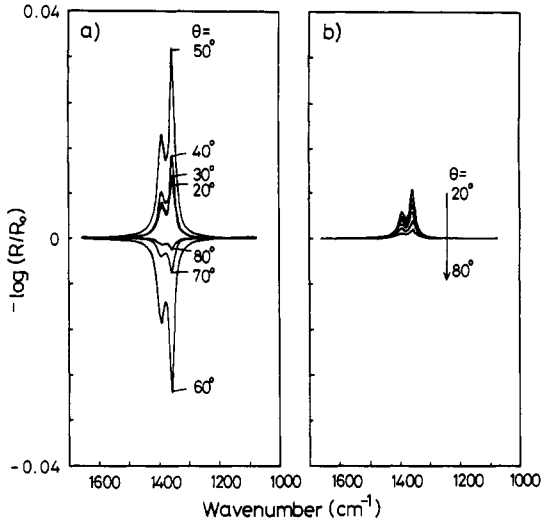

Figure 10. Simulated reflection SEIRA spectra of a model molecular layer (d_{mol} = 1 nm) on a silver film (d_{mass} = 5 nm, F = 0.9, a = 30 nm, η = 3) on BaF_2 for p- and s-polarizations (a and b, respectively).

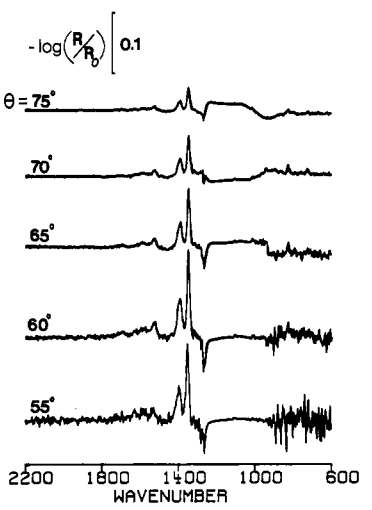

Figure 11. p-polarized silver-overlayer reflection SEIRA spectra of a 4-nm-thick PNBA film on a microscope slide glass. The thickness of the silver overlayer is 5 nm.

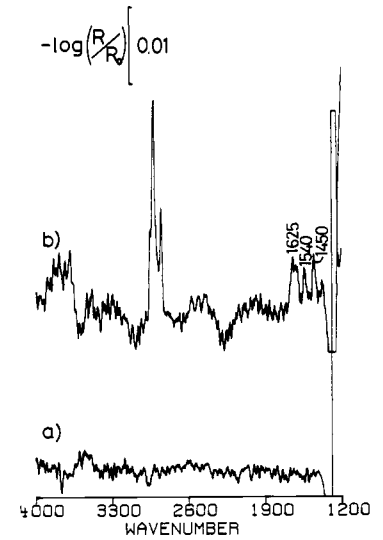

Figure 12. p-polarized infrared reflection spectra of a LB monolayer of poly(*n*-dodecylacrylamide) on a slide glass before (a) and after (b) silver deposition. The thickness of silver overlayer is 5 nm. The angle of incidence is 65°.

(Figures 2 and 3). However, the band distortion is not simulated in the model calculation. We note here that calculated SEIRA spectra change greatly depending on the shape, size, and aggregation parameters of the metal islands (α, η, and F), especially on η.[12] Figure 10 shows the calculated spectra using parameters of a = 30 nm, η = 3, and F = 0.9. The spectra are the upside down and reverse of those in Figure 8. In addition, the peak positions are slightly shifted to higher wavenumbers (1393 and 1356 cm^{-1}). If we take a sum of the calculated spectra in Figures 8 and 10, the observed distorted band shape can be simulated. Therefore, inhomogeneity of the metal-island structure probably causes the band distortion. Actually, the metal islands are not uniform in size, shape, and distribution, as can be seen in Figure 6.

The observed SEIRA intensity on Ge is one-fifth of that on BaF_2 (cf. Figures 2 and 3b). In order to see the substrate dependence, we carried out the calculations also for Ge and Si substrates using the same parameters as in Figure 8, and found that the peak intensity decreases as the refractive index of the substrate increases. The calculated intensity for the Ge substrate was a half of that for the BaF_2 substrate. The slight discrepancy in the relative intensity between the calculation and experiments probably arises from the disregard of difference in island structures on Ge and BaF_2 in the calculation. Detailed studies of the relation between the metal-island structure and enhancement are required. However, we can conclude that low refractive substrates are "optically" favorable for SEIRA experiments.

We carried out the calculations also for the case that the voids between metal particles are filled with molecules (see Figure 7a) by increasing d_{mol} or by taking $\epsilon_h = \epsilon_d$. However, band intensities were almost unchanged. This is because the absorption enhancement decreases rapidly as the distance from the metal surface increases.[10,12]

C. Metal-Overlayer Configuration. The external reflection SEIRA spectra of PNBA were obtained also with silver-overlayer configuration on BaF_2, Ge, glass, and polymer substrates. The polarization and θ dependence of the metal-overlayer SEIRA spectra were the same as those of the metal-underlyaer spectra shown above. We show in Figure 11 the p-polarized silver-overlayer reflection SEIRA spectra of a 4-nm-thick PNBA film on a slide glass. The thickness of the silver overlayer is 5 nm. The refractive index of the glass is about 1.5 and the pseudo-Brewster angle is about 56°. As is the case in metal-underlayer configuration, the positive absorption bands are observed at incident angles higher than θ_B. The negative band at 1270 cm^{-1} is not of PNBA but a ghost that was produced by the background subtraction procedure. For $\theta < \theta_B$, the absorption was negative (not shown). These results indicate that our electromagnetic model proposed for metal-underlayer configuration is applicable also for metal-overlayer configuration. This is not surprising because metal-overlayer films do not differ greatly from metal-underlayer films in the composite-film approximation.

In order to show that monolayer sensitivity can be achieved by the use of the SEIRA technique, we measured a LB monolayer of poly(*n*-dodecylacrylamide) transferred onto a slide glass. Figure 12a shows the p-polarized reflection spectrum of the LB film, where no bands are observed. Spectrum b in the figure was obtained after evaporation of a 5-nm-thick silver film on the sample. The spectrum was measured at θ = 65°. Although the enhancement was largest around θ_B, the best S/N ratio was obtained at an angle larger than θ_B. We see the bands assigned to alkyl and amid groups around 2900 and 1500 cm^{-1}, respectively. The SEIRA spectrum was almost the same as the transmission spectrum of the 20-monolayer LB film on CaF_2. The enhancement factor of 20 estimated from a comparison with the transmission

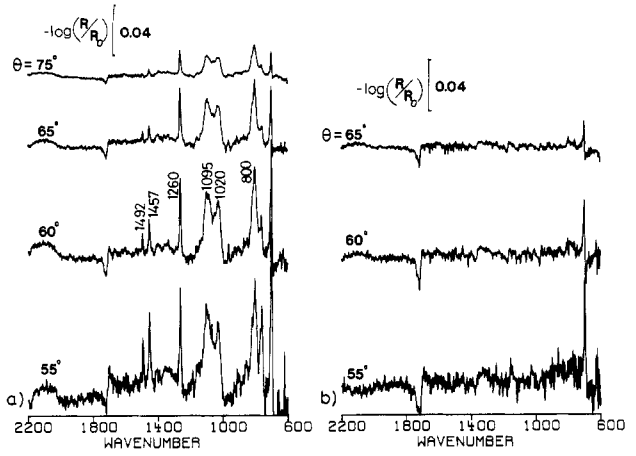

Figure 13. p-polarized infrared reflection spectra of a 5-nm-thick PDMS film on ABS resin with (a) and without (b) a 5-nm-thick silver overlayer.

spectrum is in good agreement with the model calculation described in section C.

D. Surface Analysis of Polymers with Metal-Overlayer SEIRA. Considerable attention has been focused on surface analysis of polymers in connection with adhesion, lubrication, degradation, and biocompatibility. Different from the studies of metallic surfaces, the ATR technique is more effective for polymers than the external reflection technique because of their low reflectivities.[32,33] Unfortunately, however, the conventional ATR technique is not surface sensitive because the penetration depth of the infrared radiation is an order of wavelength. Therefore, the separation of week surface signals from strong bulk signals is quite difficult. Furthermore, the sensitivity is not high enough to characterize organic films of subnanometer thickness.

Nakao and Yamada[7] solved these problems by using ATR SEIRA, where they evaporated very thin metal films on the polymers and then pressed a Si prism on them. Nishikawa et al.[9] measured ATR SEIRA spectra by placing a metal-coated ATR prism on top of polymers. Despite these efforts, there remains the problem that the ATR SEIRA technques can be applied only to soft polymers having smooth surfaces because good optical contact between the ATR prisms and samples is required.

We applied external reflection SEIRA spectroscopy to the detection of very thin films of PDMS on ABS resin. PDMS is widely used as a mold-releasing agent in the polymer-forming process. Since the remainder of the agent on the surfaces causes several problems in the latter surface treatments, surface analysis is practically important. The surface of the ABS resin plate we used was very rough of an order of a few hundred micrometers, and therefore, the ATR SEIRA technique is not applicable.

Figure 13a shows the p-polarized external reflection SEIRA spectra of a 5-nm-thick PDMS film on the ABS resin. The thickness of the silver overlayer was 5 nm. The strong bands of PDMS are observed clearly. The 1095- and 1020-cm^{-1} bands in the spectra are assigned to the Si–O–Si stretching modes. The CH_3 deformation and rocking modes are observed at 1260 and 800 cm^{-1}, respectively. We also see the bands of the substrate at 1492 and 1457 cm^{-1}. The 1730-cm^{-1} band is attributed probably to a plasticizer in the resin. It is clear from a comparison with the reflection spectrum without a metal film (Figure 13b) that both the bands of PDMS and the substrate are remarkably enhanced by the metal overlayer. Since the spacial range of the absorption enhancement is very short (a few monolayer thicknesses from metal surface),[10,12] the presence of the enhanced substrate bands suggests that the evaporated metal particles are in close contact with the substrate surface. This is probably because the metal particles are penetrating into the PDMS film or the PDMS film is discontinuous.

E. Advantages and Limitations of the Technique. We have shown above that infrared reflection spectra of very thin organic films on transparent and translucent substrates can be obtained quite easily by evaporating thin silver films on them. The SEIRA technique has higher sensitivity than the conventional external reflection and ATR techniques for these low reflective substrates. Although the technique described in the present study is a modification of the ATR SEIRA technique, it has the great advantage that an ATR prism is not required. Therefore, curved or rough surfaces can be analyzed. In addition, since SEIRA spectra can be obtained at normal incidence ($\theta = 0°$), as shown in Figure 9, external reflection SEIRA spectroscopy is more favorable than ATR SEIRA spectroscopy for micro surface analysis using an infrared microscope.

It must be noted however that the SEIRA technique has some disadvantages. Many organic films, including the LB and PDMS films used in the present study, were stable against the metal deposition. However PNBA, as an example, reacts with the metal surface and the spectra are changed greatly from the original molecule. Some molecules might be decomposed or volatilized during the metal deposition in vacuum. Therefore, we must be careful in the spectral analysis and sample preparation. In addition, SEIRA intensity is not a linear function of the thickness of organic films[10,12] and greatly depends on metal-island structure as described above. Therefore, more detailed studies are required for quantitative analysis.

Despite these limitations, the SEIRA technique is still promising because surface analytical tools for insulators are very limited. Photoelectron spectroscopies, for example, are not useful because of charge-up of the samples. The reactions, degradation, and vaporization of the sample molecules during metal evaporation is not a serious problem in most cases. We note that the metal-overlayer technique is used also in sample preparations for inelastic electron tunneling spectroscopy (IETS), and many molecules have been measured.[34] It is now well established that IETS is a powerful tool for trace analysis and surface studies. In addition, reactions of the molecules with the evaporated metals will be avoided by using gold instead of silver. The decomposition of surface molecules during the metal deposition will be avoided or minimized by placing the substrate far from the evaporation source and by limiting the metal thickness to as thin as possible. The SEIRA spectra having S/N ratios good enough to characterize subnanometer thick organic films were obtained with metal thicknesses less than 5 nm.

ACKNOWLEDGMENT

The Langmuir–Blodgett film was prepared by Prof. T. Miyashita and J. Sasaki of Tohoku University. The scanning electron micrographs were taken by T. Nagasawa and T. Fujita of Konica Corp. Their cooperation and consultation are greatly appreciated. M.O. gratefully acknowledges financial support by Grants-in-Aid for Scientific Research from The Ministry of Education, Science, and Culture of Japan and by the Miyagi Foundation for Promotion of Industry.

(32) Ohta, K.; Iwamoto, R. *Anal. Chem.* **1985**, *57*, 2491–2499.
(33) Grobe, G. L., III; Nagel, A. S.; Gardella, J. A., Jr.; Chin, R. L.; Salvati, L., Jr. *Appl. Spectrosc.* **1988**, *42*, 980–989.
(34) For a review: Fulde, P. *Inelastic Electron Tunneling Spectroscopy*; Springer-Verlag: Berlin, 1978.

RECEIVED for review September 1, 1992. Accepted November 24, 1992.